UDK 546.82:532.64
Original scientific article/Izvirni znanstveni članek

ISSN 1580-2949
Mater. Tehnol.

INVESTIGATION OF LASER PARAMETERS ON Ti-6AL-4V TITANIUM ALLOY FOR DIMPLE GENERATION USING HYBRID OPTIMIZATION TECHNIQUE

RAZISKAVE PARAMETROV LASERJA ZA GENERIRANJE JAMIC NA ZLITINI Ti-6Al-4V Z UPORABO HIBRIDNE OPTIMIZACIJSKE TEHNIKE

Ayanar R.[1*], Saravanan K.G.[2]

[1]Mechanical Engineering, Thiagarajar Polytechnic College, Salem - 636 005
[2]Mechanical Engineering, Sona College of Technology, Salem-636005

Prejem rokopisa – received: 2024-10-16; sprejem za objavo – accepted for publication: 2025-06-19

doi:10.17222/mit.2024.1329

Surface-modified Ti-6AL-4V titanium alloy finds application as a biomedical implant. There are varieties of processes existing for surface modification, and laser surface texturing is one among them. In this research micro dimples are generated on the titanium alloy using a laser, and the effect of laser parameters on the contact angle (A) and dimple diameter (D) is studied. The variables, such as dimple distance (DD)in μm, laser power (E) in watts, laser frequency (F) in kHz, and standoff distance (SOD) in mm, were considered as input factors. L18 Orthogonal array was considered as an experimental plan, and Criteria Importance through Intercriteria Correlation (CRITIC) - Grey Relational Analysis (GRA) was used to analyse the result. Using the CRITIC method, the weights for the contact angle and dimple diameter were evaluated as 0.48 and 0.52, respectively. Based on GRA, the optimal combination is 100μm, 30 W, 60 kHz, and 227mm for better output performance, and as per Analysis of Variance (ANOVA), dimple distance and laser power are the primary parameters that determine the contact angle and dimple diameter; they contribute a higher proportion of 31.85% and 38.48%, respectively.

Keywords: Titanium alloy; contact angle; dimple diameter; CRITIC; Grey Relational Analysis; ANOVA

Površinska modifikacija titanovih zlitin tipa Ti-6AL-4V se lahko uporablja za biomedicinske vsadke (implante). Obstaja vrsta postopkov za modifikacijo površin med katerimemi je tudi lasersko teksturiranje. V tem članku avtorji opisujejo raziskavo laserske izdelave jamic mikrometerske velikosti in vpliv parametrov laserja na kontaktni kot oziroma kot omakanja (A) ter premer jamic (D). Kot vhodne parametre za oceno vpliva so uporabili naslednje spremenljivke: razdaljo med jamicami (DD) v mikrometrih, moč laserja (E) v vatih, frekvenco laserja (F) v kHz in oddaljenost vira (SOD) v mm. Za analizo rezultatov so uporabili eksperimentalni načrt z ortogonalno matriko tipa L18 in metodo pomembnosti kriterijev z medkriterijsko korelacijo (CRITIC; angl.: Criteria Intercriteria Correlation) s sivo relacijsko analizo (GRA; angl.: Grey Relational Analysis). Z uporabo metode CRITIC so uteži za kotaktni kot in premer jamic podale vrednosti 0,48 oziroma 0,52. Na osnovi GRA so dobili optimalno kombinacijo izhodnih vrednosti 100 μm, 30 W, 60 kHz in 227 mm. Z variančno analizo (ANOVA; angl.: Analysis of Variance) so ugotovili, da sta razdalja med jamicami in moč laserja osnovna parametra, ki določata kontaktni kot in premer jamic ter prispevata največji delež celote (31,85% in 38,48%).

Ključne besede: titanove zlitine, kontaktni kot, premer jamic, CRITIC, siva relacijska analiza, ANOVA

1 INTRODUCTION

Applications for titanium (Ti-6Al-4V) alloy are numerous in the fields of biomedicine, energy, marine engineering, aircraft, and defence. Ti-6Al-4V alloy material finds an important place in biomedical implants, where the surface functionality must be modified in order to better accomplish the goal since surface characteristics are crucial in increasing the erosion resistance of materials. Surface texturing has been extensively used in recent years to raise surface functionalities and change the surface characteristics of a variety of materials. Thanigaivelan et al. have generated laser dimples on the 316L stainless steel; they first fabricated the dimples and electrochemically treated the dimpled surface. They found the surface roughness is 2.64 μm, the surface hardness is 538.21 N/mm^2, and the contact angle is 111.1° when the lowest dimple distance of 150 μm, laser power of 14 W, supply electrode voltage of 4 V, and electrolyte concentration of 10 g/L of $NaNO_3$ were combined.[1] Ganesan and Rajasekaran have optimised the laser parameters on output performance for 316L stainless steel; the best laser parameter settings are 15 kHz frequency, 12 W average power, and 1500 ns pulse length. Based on the Analysis of Variance (ANOVA) results, average power is the most significant component, accounting for 86.40 % of the performance measures (average depth, average dimple diameter, and average dimple distance).[2] Health Royal Hermonson has generated a laser-textured surface on 316L SS and further coated it with powdered HA using an electrochemical process, and its surface underwent a series of tests to determine its biocompatibility.

*Corresponding author's e-mail:
phdscholarayanar@gmail.com (Ayanar R.)

The results of the measurement of contact angle reveal information on the substrate's wettability. The evaluated sample that was most appropriate for bone implantation had a 98 % laser energy input, a 40.45° contact angle, and a 75.976 μm HA coating thickness. Pfleging et al. have used an ArF laser to create both linear and dimpled textures on Ti-6Al-4V. The dimple textures have a diameter of 60 μm and are evenly distributed. Compared to as-received Ti-6Al-4V (37 mN/m), the total surface energy is enhanced due to dimple (67.6 mN/m) and decreased due to linear (29.6 mN/m) texturing.[4] In Conradi's research, laser-surface texturing is demonstrated as a surface modification technique that modifies the Ti-6Al-4V morphology by introducing dimples, crosshatches, and lines. They concluded that laser surface texturing provides a workable way to improve the Ti-6Al-4V alloy's tribological characteristics. By resolving wear and friction issues under varied operating conditions, it increases the alloy's potential for a wide range of industrial applications.[5] Woźniak et al. investigated the tribological behaviour of the Ti-6Al-4V alloy with laser texture. Under lubricated test conditions, the surface texture improved the Ti-6Al-4V alloy's wear behaviour.[6] Liu et al. in their study, to achieve various morphologies, the titanium alloy is subjected to laser surface texturing treatment using varying pulse counts, powers, pulse widths, and scan periods. They came to the conclusion that whereas low power is more likely to create bumps regardless of pulse width, high power plus low pulse width can result in deeper pits.[7] The impact of various laser-textured Ti6Al4V alloy surface topologies on enhancing wettability and tribology features has been documented by Velayuthaperumal & Radhakrishnan.[8] According to the study, the laser-textured surface's surface oxidation was demonstrated by the presence of carbon (11.7 %) and oxygen (22.9 %) in an EDS examination. The development of hydrophilicity on the textured surfaces has been demonstrated by the wettability analysis. With a textured density of 58 % and the smallest contact angle of 51.5°, the moat pattern surface has the highest density. Madapana et al. employed electrochemical impedance spectroscopy in a simulated body fluid, and the detailed corrosion behaviour of ultrafast laser-surface-structured Ti-6Al-4V is investigated and associated with surface properties. In the presence of a thin oxide layer, laser structuring produces a topographically changed surface with periodic surface patterns.[9] This work aims to create laser-textured dimple arrays on Ti-6Al-4V under different laser settings, and assess the surface wettability (contact angle) and dimple sizes. Using a Taguchi L_{18} experimental design, investigate how processing parameters (dimple spacing, average power, pulse frequency, and standoff distance) affect these two responses and optimise the laser parameters for multi-criteria performance using a hybrid Criteria Importance through Intercriteria Correlation (CRITIC)-Grey Relational Analysis (GRA), discovering the parameter values that best achieve the required balance of contact angle and dimple size. In addition, analyse parameter significance using analysis of variance (ANOVA) to determine which laser settings have the most impact on surface wettability and texture geometry.

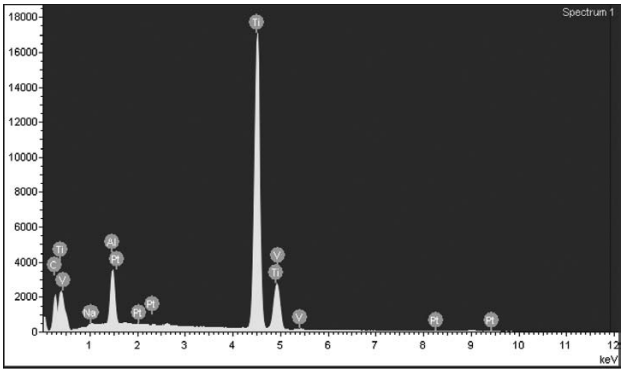

Figure 1: EDS spectrum portray the Ti-6Al-4V alloy elements

2 EXPERIMENTAL PART

As received, Ti-6Al-4V alloy of size 25 mm × 25 mm × 3 mm was utilised as a workpiece. With a resolution of 137 eV, Horiba EMAX energy dispersive X-ray spectroscopy (EDS) is used to verify the composition of the alloy. **Figure 1** and **Table 1** present the EDS and the elemental composition of the Ti-6Al-4V alloy. EDS was used to analyze a Ti-6Al-4V alloy. The Ti-6Al-4V alloy, Brinell hardness value ranges from 330-375BHN and has thermal conductivity of 6.7 W/mK. The melting point is measured as 1604–1660 °C. A typical alpha-beta titanium alloy used in biomechanical and aeronautical applications, such as implants and prostheses, is Ti-6Al-4V, generally referred to as TC4 or ASTM Grade 5.10 It has a high specific strength and exceptional resistance to corrosion. Nevertheless, it becomes necessary to alter the surface characteristics of Ti-6Al-4V for particular applications where decreased friction, improved biocompatibility, or resistance to environmental deterioration is crucial.[11]

Table 1: Elemental composition of Ti-6Al-4V alloy

Element	Weight %	Atomic %
C K	13.92	38.07
Na K	0.46	0.65
Al K	5.11	6.22
Ti K	77.18	52.94
V K	3.27	2.11
Pt M	0.07	0.01
Total	100.00	

An MLSF60 model, made by Meera Laser Solutions Pvt. Ltd., a 60-watt open-type fibre laser marking apparatus, was used in the experiment. Tamil Nadu, India's Chennai, was where the machine was found. Utilising different laser energy and dimple distances, each speci-

men were micro-texturised. Anti-scratch polymer foils were carefully applied to the specimens prior to texturing in order to prevent dirt buildup and oxidation. 10 mm by 10 mm was the size of the texturing area. **Table 2** present the laser parameters, levels and experimental design. L_{18} orthogonal array (OA) is used for the experiments, and performance measures are provided in the table. A contact angle goniometer (Model: HO-IAD-CAM-O1A, Make: Holcmarc, NIT Calicut) and deionised water were used to assess the specimens' contact angle and diameter of dimple as performance metrics. On each sample, three separate sites were used to administer 6 µL droplets. For every specimen, an average of three contact angle measurements was calculated in order to minimise measurement error. Using a non-contact 3D optical profilometer (Alicona Bruker, Model: InfiniteFocus G5, DST-FIST Lab, NIT Calicut, Kerala, India), the dimple's diameter was determined. The specimens were cleaned for thirty minutes before measurement with acetone and deionised water, assisted by an ultrasonicator. The goal of this pro-

Table 2: OA experimental design

Sl.No	DD	E	F	SOD	Contact angle (θ) (A)	Dimple Diameter (µm) (D)
1	100	30	40	223	85.00	44.11
2	100	45	50	225	75.00	47.05
3	100	58.8	60	227	69.00	54.94
4	150	30	40	225	72.00	52.94
5	150	45	50	227	65.00	55.88
6	150	58.8	60	223	61.00	58.82
7	200	30	50	223	68.00	61.76
8	200	45	60	225	66.00	64.7
9	200	58.8	40	227	61.00	67.64
10	100	30	60	227	90.00	46.94
11	100	45	40	223	76.00	48.05
12	100	58.8	50	225	59.00	58.82
13	150	30	50	227	74.00	61.76
14	150	45	60	223	71.00	63.94
15	150	58.8	40	225	61.00	67.64
16	200	30	60	225	70.00	70.58
17	200	45	40	227	65.00	73.52
18	200	58.8	50	223	61.00	76.47

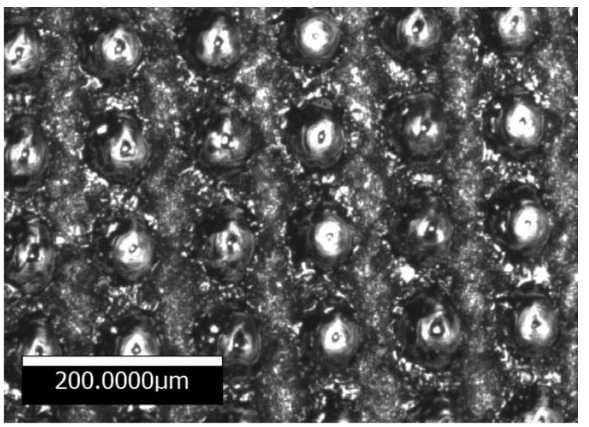

Figure 2: Laser surface texturing with 100µm distance

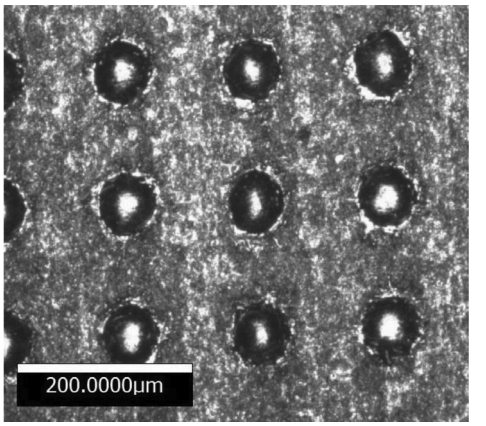

Figure 3: Laser surface texturing with 150µm distance

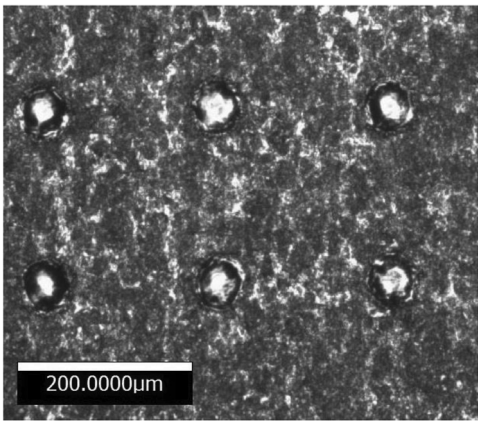

Figure 4: Laser surface texturing with 200µm distance

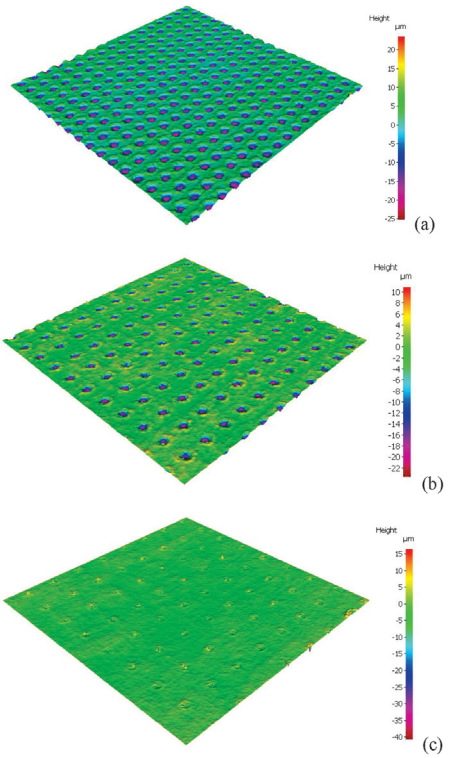

Figure 5: 3D surface profile of textured sample with dimple distance of: a) 100 µm, b) 150 µm, c) 200 µm

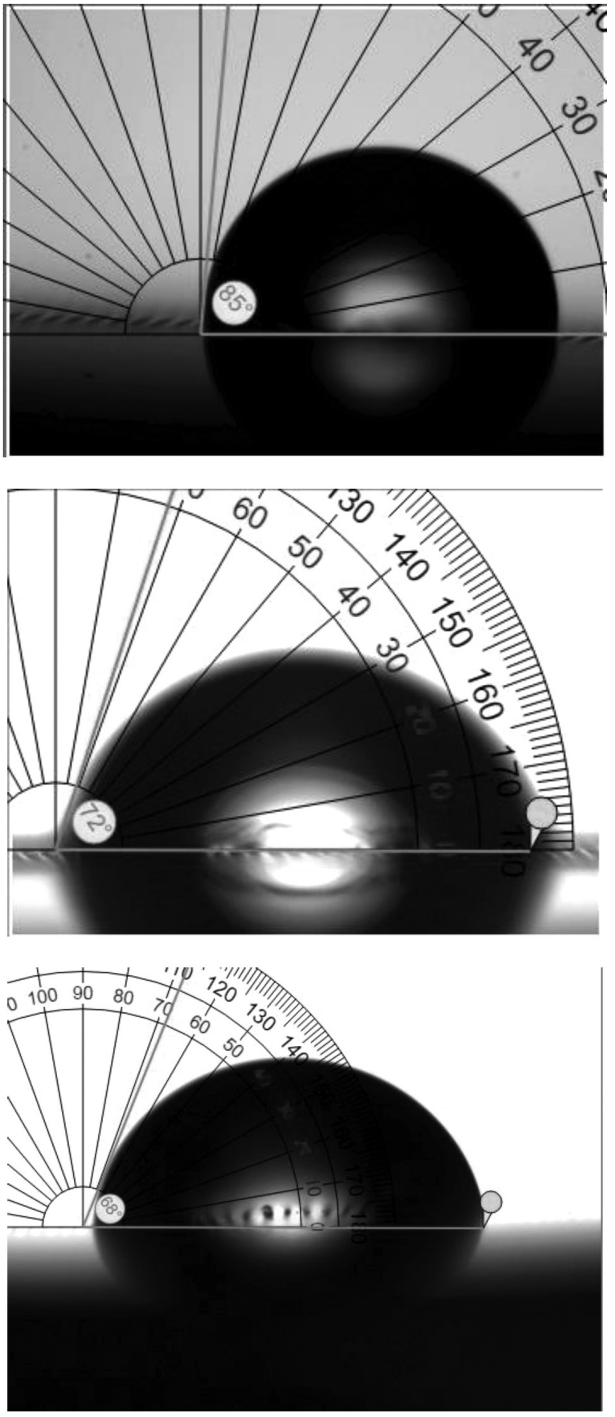

Figure 6: Contact angle images for: a) 100 µm dimple distance, b) 150 µm dimple distance, c) 200 µm dimple distance

cedure was to get rid of the molten slag that was created after laser surface texturing.

Figures 2 to **4** show the laser textured sample with 100 µm,150 µm & 200 µm dimple distance respectively. **Figures 5a** to **5c** presents the 3D surface profile of textured sample with three dimple distance. **Figure 6** depicts the contact angle images of the sample with 100 µm, 150 µm & 200 µm dimple distance respectively.

3 CRITERIA IMPORTANCE THROUGH INTERCRITERIA CORRELATION –GREY RELATION GRADE (GRG) METHOD

The CRITIC-GRG technique is a hybrid approach that uses the CRITIC method to generate criteria weights and subsequently apply the GRA technique to rank the alternatives. Diakoulaki et al. were instrumental in evolving this CRITIC technique, which extract the entire data present in the evaluation criteria by examining the assessment matrix. Here, criterion's association with other criteria and standard deviation were considered to assess the criterion weights.[12]

Let, D = $[A_{ij}]_{xxy}$, be the initial matrix, "x" stand for the no. of alternatives, "y" designate the no. of criteria, and A_{ij} is the i^{th} alternative's performance measure in relative to the j^{th} criterion.

Table 4 displays the values of equation (1), which is used to normalize the original decision matrix using the CRITIC approach.[13–15]

$$N_{ij} = \frac{A_{ij} - A_j^{worst}}{A_j^{best} - A_j^{worst}} \quad (1)$$

where A_{ij} signify the normalized value of the i^{th} design on the j^{th} response.

The weights allocated to each criterion by evaluating the standard deviation. The weight of the j^{th} criterion η_j can be established by means of the following technique.

$$\omega_j = \frac{\eta_j}{\sum_{i=1}^{n} \eta_i} \quad (2)$$

Where η_j is the sum of information there in the j^{th} criterion, can be obtain as described below:

$$\eta_j = \delta_j \sum_{i=1}^{m} (1 - \alpha_{ij}) \quad (3)$$

α_{ij} signify the correlation coefficient between the j^{th} and i^{th} criteria, δ_j represent the standard deviation of the j^{th} criterion.

The weights for every response are calculated using CRITIC method and correspond to its respective GRA relative relevance. Equation (3), calculate the correlation coefficient and standard deviation, which is applied to the array of grey relational coefficient (GRC). The calculated correlation coefficients of output performance are 1 and 0.7025 respectively. The standard deviations for every quality indicator are 0.27 and 0.30 respectively.

Next, using Equation (2), the corresponding weights for each quality attribute were resolute as 0.480 and 0.520. The GRG was also calculated by these weights.

4 MULTI-RESPONSE OPTIMIZATION USING GRA

In this study, the correlation between multiple performance measurements is taken into account while optimising the process parameters using the GRA approach.

This is where the GRA for selecting the ideal machining parameters is displayed. Due to the possibility of disparate data sequences with varying ranges and units, data pre-processing is required for GRA. Data pre-processing is also necessary when the target orientations in the sequence differ or when the sequence's scatter range is particularly large. Data pre-processing is the process of rearranging the original sequence into a more comparable one. According to Thangaivelan and Arunachalam,the experimental data are normalised within the interval of 0 to 1.[16]

Since the contact angle determines the hydrophobic properties of the laser-textured surface, the "larger-the-better" attribute is taken into account, and the contact angle's initial value is normalised using the equation that follows.

$$\alpha_i^*(t) = \frac{\alpha(t) - \min \alpha_i(t)}{\max \alpha_i(t) - \min \alpha_i(t)} \quad (4)$$

where, $\alpha^*_i(t)$ and $\alpha_i(t)$ are the series after the data pre-processing and comparability sequence correspondingly, t = 1 for contact angle i = 1, 2, 3…, 18 for experiment numbers 1 to 18.

Another crucial metric for assessing the hydrophobic properties of a laser-textured surface is the dimple diameter. For more hydrophobic qualities, the dimple diameter should be smaller; consequently, the "smaller-the-better" quality feature has been applied. The original dimple diameter sequence is normalized using equation (5).

$$\alpha_i^*(t) = \frac{\max \alpha_i(t) - \alpha_i(t)}{\max \alpha_i(t) - \min \alpha_i(t)} \quad (5)$$

where, $\alpha^*_i(t)$ and $\alpha_i(t)$ are the order after the data pre-processing and comparability series correspondingly, t = 2 for dimple diameter, i = 1, 2, 3…, 18 for experiment numbers 1 to 18. **Table 3** illustrates the normalized values for contact angle and dimple diameter.

After weight assignment and an overall evaluation of the multiple objective optimisation obtained by utilising Equation (6), the GRG shown in **Table 8** is computed by averaging the GRC.

$$\mu_j = \frac{1}{p} \sum_{q=1}^{p} \xi_i(E) \quad (6)$$

where μ_j is the GRG of j^{th} experiment and p is the no. of performance characteristics.

In terms of process parameters, the highest value of GRG represents the optimal level. An indicator of proximity to the ideal value is the computed higher GRG value. As seen in **Table 2**, the ideal combination of machining parameters for a larger contact angle and a smaller dimple diameter is 100 μm, 30 W, 60 kHz, and 227 mm.

5 EFFECT OF PROCESS VARIABLES

Figure 7 shows the effect of process variables on output performances. It can be seen from the graph that an increase in dimple distance reduces the contact angle and the dimple diameter. At shorter dimple distances, the dimples generated by the laser create more molten and solidified regions on the surface. These regions show the patterns of micro/nano streaks, needles and spherical particles on the laser-dimpled surface. While the dimple distance increases, the lack of formation of former patterns attributes to reduced hydrophobic surfaces. Moreover, it is evident from the mean effect plot that the increase in dimple distance reduces the dimple diameter. It

Table 3: Values for normalized data

Expt. Run	Normalizing		Deviation sequence		GRC		GRC × ω_i		GRG	Rank
	$\alpha^*_i(t)$	$\alpha_i(t)$	A	D	A	D	A	D		
1	0.8405	1.0000	0.0674	0.1595	0.8812	0.7581	0.4230	0.3942	0.4086	2
2	0.5073	0.9091	0.4643	0.4927	0.5185	0.5037	0.2489	0.2619	0.2554	
3	0.3191	0.6653	0.6631	0.6809	0.4299	0.4234	0.2063	0.2202	0.2133	
4	0.4257	0.7271	0.5468	0.5743	0.4776	0.4654	0.2293	0.2420	0.2356	
5	0.1959	0.6363	0.7931	0.8041	0.3867	0.3834	0.1856	0.1994	0.1925	
6	0.0673	0.5454	0.9289	0.9327	0.3499	0.3490	0.1680	0.1815	0.1747	
7	0.2980	0.4546	0.6701	0.7020	0.4273	0.4160	0.2051	0.2163	0.2107	
8	0.2310	0.3637	0.7561	0.7690	0.3981	0.3940	0.1911	0.2049	0.1980	
9	0.0638	0.2729	0.9326	0.9362	0.3490	0.3481	0.1675	0.1810	0.1743	
10	1.0000	0.9125	0.0000	0.0000	1.0000	1.0000	0.4800	0.5200	0.5000	1
11	0.5424	0.8782	0.4272	0.4576	0.5392	0.5222	0.2588	0.2715	0.2652	3
12	0.0000	0.5454	1.0000	1.0000	0.3333	0.3333	0.1600	0.1733	0.1667	
13	0.4997	0.4546	0.4724	0.5003	0.5142	0.4998	0.2468	0.2599	0.2534	
14	0.3874	0.3872	0.5910	0.6126	0.4583	0.4494	0.2200	0.2337	0.2268	
15	0.0673	0.2729	0.9289	0.9327	0.3499	0.3490	0.1680	0.1815	0.1747	
16	0.3443	0.1820	0.6365	0.6557	0.4400	0.4326	0.2112	0.2250	0.6365	
17	0.1991	0.0912	0.7898	0.8009	0.3877	0.3844	0.1861	0.1999	0.7898	
18	0.0606	0.0000	0.9360	0.9394	0.3482	0.3474	0.1671	0.1806	0.9360	

Table 4: ANOVA table

Symbol	Laser parameter	Degrees of Freedom	Sum of the squares	Mean sum of the square	F-test	% contribution
DD	Dimple distance	2	0.0407	0.02034	9.79595	31.85
E	Power	2	0.0492	0.02458	11.8352	38.48
F	Frequency	2	0.0074	0.0037	1.78134	5.79
SOD	Standoff distance	2	0.0077	0.00383	1.8431	5.99
E	Error	11	0.0228	0.00208		23.88
	Total	17	0.12775	0.00751		100

is due to the fact that during laser processing, less widening of the re-solidified zone results in small-diameter dimples.[17] An increase in laser power reduces the contact angle and dimple diameter. This phenomena was supported by Khadka Indira et al, laser irradiation with 50 W, 100 W, and 150 W power resulted in decreased contact angles compared to the as received specimen.[18] During the laser process, the height of the recast layers formed on the circumference of the dimple reduces with the laser energy due to the vapourisation ratio in the irradiated material being larger than the melting ratio.[19] The increase in laser frequency first reduces the contact angle and dimple diameter and further increases the same. Rajurkar et al, have documented that laser frequency are the important deciding factors of hydrophobicity.[20] The increase in frequency results in a lot of jagged ripples of micro/nano streaks, needles and spherical shapes. Other parameters that affect the output performance are standoff distance (SOD); the higher values of SOD show enhancement of contact angle and dimple diameter. The increase in SOD results in irregular patterns of dimples; at lower SOD, small dimples were formed, followed by irregularly shaped craters. The increase in SOD results in enlarged shallow circular dimples, attributing to the increased dimple diameter.[21] Moreover, based on the literature, the SOD of 223.12mm, shows the contact angle of 159.00.[22]

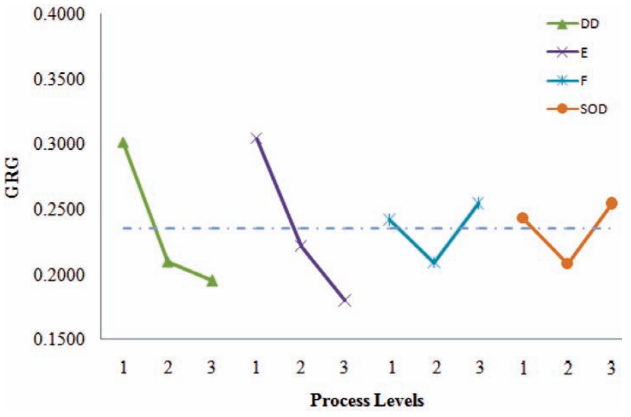

Figure 7: Mean effect plot for GRG

5.1 ANOVA

An ANOVA analysis is conducted to investigate the impact of a process parameter on a performance attribute. To determine how process factors affect something, add up all of the squared variances. The critical process variable that influences the quality of the output is forecasted. Additionally, to determine the impact of laser parameters on the performance characteristic, the Fisher's F test is conducted.[23] **Table 9** displays the GRG-ANOVA. Dimple distance and power are the primary parameters that determine the contact angle and dimple diameter, as shown by the ANOVA table, which also reveals that they contribute a higher proportion (31.85 % and 38.48 %, respectively).

6 CONCLUSIONS

Laser array dimples were successfully formed on the Ti-6AL-4V titanium alloy using the L_{18} OA experimental plan.

The weights for the output performance were calculated using the CRITIC method as 0.48 and 0.52.

The optimal parameter combination as per the GRA for a larger contact angle and a smaller dimple diameter is 100 µm, 30 W, 60 kHz, and 227 mm.

Based on the mean effect plot increase in dimple distance reduces the contact angle and the dimple diameter.

Dimple distance and power are the primary parameters that determine the contact angle and dimple diameter, as per the ANOVA table, which also reveals that they contribute a higher proportion of 31.85 % and 38.48 %, respectively.

7 REFERENCES

[1] R. Thanigaivelan, R. M. Arunachalam, A. Nithish, S. Venkatesh, P. Naveenkumar, S. Selvaganapathy, A. S. Aravind, Optimization of Laser and Electrochemical Process Parameters for Surface Modification of Hardness and Hydrophobicity on 316L Steel. Lasers in Engineering (Old City Publishing), 45 (**2020**) 69–84

[2] S. K. Ganesan, T. Rajasekaran, Optimization of Laser Parameters and Dimple Geometry Using PCA-Coupled GRG. Journal of Mechanical Engineering/Strojniški Vestnik, 67 (**2021**) 525–533, doi:10.5545/sv-jme.2021.7246

[3] R. Health Royal Hermonson, R. Thanigaivelan, V. Kavya, K. Rathinasamy, T. Jagadeesha, Performance of electrochemically deposited hydroxyapatite on textured 316L SS for applications in

biomedicine. Surface Engineering, 39 (**2023**) 882–891, doi:10.1080/02670844.2023.2265616

[4] W. Pfleging, R. Kumari, H. Besser, T. Scharnweber, J. D. Majumdar, Laser surface textured titanium alloy (Ti–6Al–4V): Part 1–Surface characterization. Applied Surface Science, 355 (**2015**), 104–111, doi:10.1016/j.apsusc.2015.06.175

[5] M. Conradi, Laser surface texturing to improve the tribological properties of Ti alloys. Materials and Technology, 58 (**2024**), 531–536, doi:10.17222/mit.2024.1219

[6] A. Woźniak, O. Bialas, M. Adamiak, B. Hadzima, J. Szewczenko, The influence of laser texturing on the tribological behavior of titanium alloy Ti6Al4V in medical applications. Archives of Civil and Mechanical Engineering, 24 (**2024**), 1–19, doi:10.1007/s43452-024-00960-3

[7] Z. Liu, T. Niu, Y. Lei, Y. Luo, Experimental study on bumps formation textured by nanosecond laser on Ti6Al4V alloy. Biosurface and Biotribology, 9 (**2023**), 24–34, doi:10.1049/bsb2.12058

[8] S. Velayuthaperumal, R. Radhakrishnan, Effect of different laser texture configurations on improving surface wettability and wear characteristics of Ti6Al4V implant material. Journal of the Brazilian Society of Mechanical Sciences and Engineering, 45 (**2023**), 363, doi:10.1007/s40430-023-04287-7

[9] D. Madapana, R. Bathe, I. Manna, J. Dutta Majumdar, Studies on Surface Characteristics and Biocorrosion Behavior of Ultrafast Laser-Structured Titanium Alloy (Ti6Al4V). Physica Status Solidi (A), (**2024**) 2300610, doi:10.1002/pssa.202300610

[10] R. Thanigaivelan, R. M. Arunachalam, C. Madhan, R. R. Kumar, M. Muthuselvam, Impact of electrochemical passivation on Burr suppression of Ti–4Al–6V alloy during machining. Surface Engineering and Applied Electrochemistry, 55 (**2019**) 424–429, doi:10.3103/S106837551904015X

[11] I. Shivakoti, G. Kibria, R. Cep, B. B. Pradhan, A. Sharma, Laser surface texturing for biomedical applications: A review. Coatings, 11 (**2021**) 124, doi:10.3390/coatings11020124

[12] D. Diakoulaki, G. Mavrotas, L. Papayannakis, Determining objective weights in multiple criteria problems: The critic method. Computers & Operations Research, 22 (**1995**), 763–770, doi:10.1016/0305-0548(94)00059-H

[13] S. Maniraj, R. Thanigaivelan, K. Gunasekaran, K. G. Saravanan, Optimization of process parameters in electrochemical micromachining of amcs by using different techniques of weight evaluation. Advances in Materials Science and Engineering, (**2023**), 1366857, doi:10.1155/2023/1366857

[14] D. Deepa, R. Thanigaivelan, M. Venkateshwaran, M. Identifying a suitable micro-fin material for natural convective heat transfer using multi-criteria decision analysis methods. Materials Today: Proceedings, 45 (**2021**) 1655–1659, doi:10.1016/j.matpr.2020.08.480

[15] R. Thanigaivelan, S. Prakash, S. Maniraj, S. Surface Modification Techniques for Bio-Materials: An Overview. Advanced Manufacturing Techniques for Engineering and Engineered Materials, (**2022**) 19, doi:10.4018/978-1-7998-9574-9.ch003

[16] R. Thanigaivelan, R. M. Arunachalam, Optimization of process parameters on machining rate and overcut in electrochemical micromachining using grey relational analysis. Journal of scientific and industrial research, 72 (**2013**) 36–42

[17] R. Wang, S. Bai, Wettability of laser micro-circle-dimpled SiC surfaces. Applied Surface Science, 346 (**2015**) 107–110, doi:10.1016/j.apsusc.2015.04.006

[18] K. Indira, C. Sylvie, W. Zhongke, Z. Hongyu, Investigation of wettability properties of laser surface modified rare earth Mg alloy. Procedia Engineering, 141 (**2016**) 63–69, doi:10.1016/j.proeng.2015.08.1106

[19] Z. Liu, T. Niu, Y. Lei, Y. Luo, Experimental study on bumps formation textured by nanosecond laser on Ti6Al4V alloy. Biosurface and Biotribology. 9 (**2023**) 24–34, doi:10.1049/bsb2.12058

[20] A. Rajurkar, N. Darshane, G. Dengale, P. Morankar, Effect of laser process parameters on contact angle for linear and square grid micro-textured surfaces. Materials Today: Proceedings. 2023, doi:10.1016/j.matpr.2023.08.237

[21] J. Chen, D. Li, W. Yu, Z. Ma, C. Li, G. Xiang, P. Zhong, The effects of scanning speed and standoff distance of the fiber on dusting efficiency during short pulse holmium: YAG laser lithotripsy. Journal of clinical medicine, 11 (**2022**) 5048, doi:10.3390/jcm11175048

[22] J. Preetha, S. Kumar Tamang, R. Thanigaivelan, T. Jagadeesha. Optimization of laser parameters using NSGA-II for the generation of bioinspired surface. Surface Review and Letters (**2024**): 2450122, doi:10.1142/S0218625X24501221

[23] N. Rajan, M. N. S. Sri, P. Anusha, R. Thanigaivelan, S. Vijayakumar, Performance optimization of electrochemical machining parameters on aluminum metal matrix composite. Surface Engineering and Applied Electrochemistry, 59 (**2023**) 719–727, doi:10.3103/S1068375523060157